

attacked by the anion on any of the four faces (or apices) of the tetrahedron centered on the nitrogen atom. Although, by symmetry, we might expect the overall probabilities of attack to be different in the present series, this does not appear to be the case.

The dipolar shift represents a time-average shift, which is a weighted sum over a large number of possible instantaneous structures, not all of which involve intimate contact between anion and cation. For this reason, one might expect that the steric effects which determine very close approach geometries tend to be

suppressed in the dipolar shift by the averaging process. On the other hand, since the contact shift occurs only *via* direct anion-cation bonding, it is expected to reflect the local steric requirements of the ion-pairing process to a greater extent.

Acknowledgments.—The authors are grateful to the National Research Council of Canada for their financial support and to Mr. D. Weeden of these laboratories for his assistance with the conductivity measurements.

CONTRIBUTION FROM THE DEPARTMENTS OF CHEMISTRY, UNIVERSITY OF MINNESOTA, MINNEAPOLIS, MINNESOTA 55455, AND PURDUE UNIVERSITY, LAFAYETTE, INDIANA 47907

Raman Spectra of Dimethyltin(IV) and Dimethylthallium(III) in Single Crystals and Solutions. Carbon-Tin and Carbon-Thallium Derived Bond Polarizabilities^{1,2}

By VIRGINIA B. RAMOS AND R. STUART TOBIAS*

Received February 8, 1972

Raman spectra have been collected with relatively large single crystals of $(\text{CH}_3)_2\text{SnF}_2$, and they are in agreement with previous assignments of the vibrations. Relative values for the components of the derived polarizability tensors for the 531-cm^{-1} Sn-C symmetric stretching and the 114-cm^{-1} rotatory lattice modes have been measured. From the data on the Sn-C stretching mode, the ratio of the perpendicular and longitudinal components of the tin-carbon derived bond polarizability, α'_p/α'_l , was calculated to be 0.227. Limited data also were collected from single crystals of $(\text{CH}_3)_2\text{TlBr}$, and the vibrations were assigned. The depolarization ratio computed from the $(\text{CH}_3)_2\text{SnF}_2$ crystal tensor components, $\rho = 0.24 \pm 0.01$, was the same within the experimental error as the value obtained for $(\text{CH}_3)_2\text{Sn}^{2+}(\text{aq})$ by measurements on aqueous solutions of $(\text{CH}_3)_2\text{Sn}(\text{ClO}_4)_2$, $\rho = 0.22 \pm 0.02$, indicating that the electron distribution in the $(\text{CH}_3)_2\text{Sn}^{\text{IV}}$ moiety is very similar in both cases. The experimental depolarization ratio for $(\text{CH}_3)_2\text{Tl}^+(\text{aq})$ obtained by measurements on aqueous $(\text{CH}_3)_2\text{TlClO}_4$ also was 0.22 ± 0.02 indicating that α'_p/α'_l is the same for tin(IV)-carbon and thallium(III)-carbon bonds in the cations. A comparison of the crystal and solution spectra suggests that the lowest frequency solution mode in each case is better described as a libration than as a skeletal deformation mode.

Introduction

Raman spectroscopy has proved to be especially useful in the study of the stereochemistry of organometallic compounds because of the high intensity of both the metal-carbon stretching vibrations and the internal vibrations of alkyl groups. In a qualitative sense, the stretching of covalent bonds leads to relatively intense Raman scattering, while highly polar bonds give only weak scattering. Discussions of the relation between Raman intensities, molecular structure, and chemical bonding normally are framed in terms of derived bond polarizabilities, $(\partial\alpha/\partial r)$, where α is the ionic or molecular polarizability and r is the bond stretching coordinate. Unfortunately, there are very few data available on bond polarizabilities, and consequently it is very difficult to treat Raman intensities in any quantitative way.

The bond polarizabilities are computed from the derived polarizability for a vibration, $\alpha_j' = (\partial\alpha/\partial Q_j)$ where Q_j is the normal coordinate. The square of the derived polarizability is proportional to the experimentally observed band intensity. A clear discussion of the polarizability theory is given by Brandmüller

and Moser.³ The bond polarizabilities most often have been related to bond order using the approximate equation of Long and Plane,⁴ and the applications to inorganic systems have been reviewed recently by Spiro.⁵

With unoriented samples, *i.e.*, gases, liquids, and solutions, only the derived polarizability tensor invariants, the quantities which are independent of the relation between molecular and laboratory coordinates,⁶ can be determined. This limitation can be removed by the use of an oriented single crystal where each of the derived polarizability tensor components can be examined independently.

In this work, relative values have been measured for the derived polarizability tensor components for the totally symmetric tin-carbon stretching vibrations of $(\text{CH}_3)_2\text{SnF}_2$ which are equivalent to the values for the tin-carbon derived bond polarizabilities. From these data, the depolarization ratio of $(\text{CH}_3)_2\text{SnF}_2$ can be computed for comparison with the corresponding vibration of $(\text{CH}_3)_2\text{Sn}^{2+}$ in aqueous solution and the dimethyltin(IV) moiety in other compounds. The Raman spectrum of a powder sample of $(\text{CH}_3)_2\text{SnF}_2$

* To whom correspondence should be addressed at Purdue University.

(1) Supported, in part, by the National Science Foundation, Grant GP-23208, and by the donors of The Petroleum Research Fund, administered by the American Chemical Society. Work done at Purdue University.

(2) Taken from a thesis submitted by V. B. R. to the Graduate School of the University of Minnesota in partial fulfillment of the requirements for the Ph.D. degree, 1972.

(3) J. Brandmüller and H. Moser, "Einführung in die Ramanspektroskopie," D. Steinkopff, Darmstadt, 1962, Chapter 4.

(4) T. V. Long, II, and R. A. Plane, *J. Chem. Phys.*, **43**, 457 (1965).

(5) T. G. Spiro, *Progr. Inorg. Chem.*, **11**, 1 (1970).

(6) Intensities of unoriented samples have been reviewed by R. E. Hester in "Raman Spectroscopy," Vol. 1, H. A. Szymanski, Ed., Plenum Press, New York, N. Y., 1967, Chapter 4.

was originally determined for comparison with the spectrum of $K_2[(CH_3)_2SnF_4]$.⁷ With the $[(CH_3)_2SnF_4]^{2-}$ ion, the Raman-active totally symmetric Sn-F stretching vibration gave rise to scattering too low in intensity to be measured indicating quite ionic tin-fluorine interactions. The frequencies associated with the vibrations of the dimethyltin(IV) moiety of $(CH_3)_2SnF_2$ are similar, and Hobbs and Tobias⁷ suggested that the absence of measurable scattering from Sn-F stretching had the same basis as with the $[(CH_3)_2SnF_4]^{2-}$ anion. As has been pointed out by Goldstein and Unsworth,⁸ $(CH_3)_2SnF_2$ has no Raman-active Sn-F stretching modes because of the sheet-like polymeric structure which results from tin-fluorine interactions. The unit cell is centric,⁹ and trans Sn-F bonds are constrained to vibrate out of phase. In addition, measurements are reported here for a $(CH_3)_2TlBr$ single crystal which has a structure¹⁰ closely related to $(CH_3)_2SnF_2$, and these also are compared with solution data.

Experimental Section

Dimethyl Difluoride.—The compound was prepared by reaction of $(CH_3)_2SnO$ obtained from M and T Chemicals, Rahway, N. J., with aqueous HF,⁶ and the product was recrystallized from 48% HF. *Anal.* Calcd for $C_2H_6SnF_2$: C, 12.9; H, 3.23; F, 20.3. Found: C, 12.5; H, 3.2; F, 20.4. Single crystals were grown by slow evaporation of unsaturated solutions of $(CH_3)_2SnF_2$ in HF. Crystals 1–2 mm thick and 2–4 mm on each side could be obtained over a period of 6–8 weeks. The well-developed flat faces correspond to the (001) faces, and an X-ray diffraction pattern of a single crystal revealed that the edges coincided with the crystallographic $a(b)$ directions. Crystals with no visible imperfections were selected, and in some cases smaller crystals were cut from the larger single crystals. The crystal was glued along either the (100) or (010) face onto a standard two-circle goniometer head. Alignment was done using Laue transmission photographs, and the orientations are believed to be accurate to $\pm 0.5^\circ$.

Dimethyltin Perchlorate Solutions.—Dimethyltin oxide was dissolved in a slight excess of 2 M HClO₄ to give a 1 M solution.

Dimethylthallium Bromide.—Dimethylthallium iodide was prepared by the method of Gilman and Jones.¹¹ The iodide was reacted with aqueous AgNO₃ to yield the aquo cation, and $(CH_3)_2TlBr$ was precipitated by adding NaBr. Single crystals were grown by slow evaporation of pyridine and aqueous solutions. The flat tetragonal faces were identified as the (001) faces from the crystal morphology, and the crystals were oriented on the goniometer head visually.

Dimethylthallium Perchlorate Solutions.—Dimethylthallium hydroxide was prepared by reacting $(CH_3)_2TlI$ with Ag₂O in water. The resulting solution was neutralized with a slight excess of 2 M HClO₄ giving a 0.3 M solution.

Raman Spectrophotometer.—The spectrophotometer consisted essentially of a Spex 1400 double monochromator and three laser sources: Spectra Physics Model 112 He-Ne, Coherent Radiation Model 52 Ar⁺, and Control Laser Orlando Model 400 Ar⁺. Detection was by a thermoelectrically cooled (-20°) EMI 9558A photomultiplier with magnetic lens assembly to give dark counts of about 2 cps at 1600 V. Analog and digital data were displayed on a recorder and punched on paper tape, respectively. The electronics included a Canberra Model 1405 preamplifier, 1415 RC amplifier, and 1431 single channel analyzer. The analog signal was provided by a Canberra 1480 linear ratemeter and recorded with a Phoenix Instruments Ratio Recorder (modified Brown-Honeywell recorder). Digital data were collected as counts per wavelength interval while scanning continuously. The wavelength interval was measured as a preset number of pulses from a Theta shaft encoder coupled to the grating drive. These pulses served as the time base for an

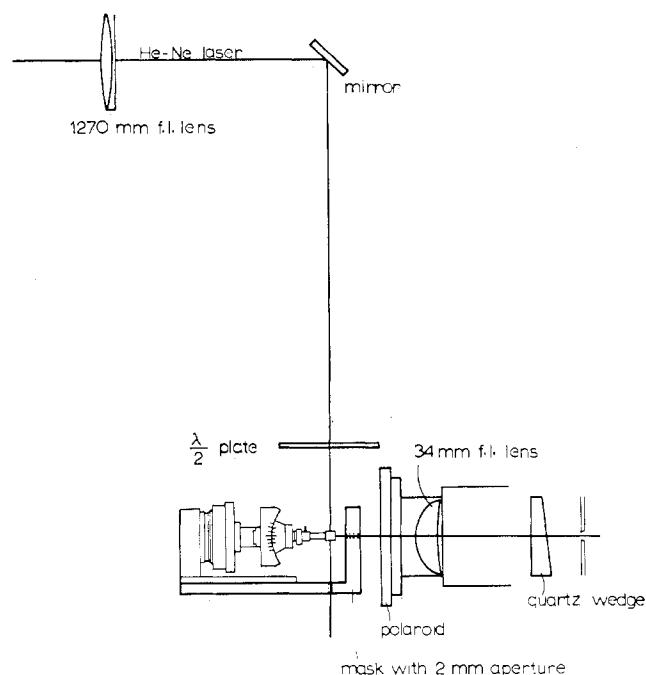


Figure 1.—Optical setup for oriented single-crystal spectra.

Ortec Model 434 buffered digital ratemeter which was connected in parallel with the Canberra linear ratemeter. An Ortec Model 707 buffered scaler was used to monitor the wavelength by counting the shaft encoder pulses. Data were printed and punched as pairs giving cumulative shift encoder pulses and photon counts for each predetermined interval. Output was via an Ortec 432 printout control and a Model 222 page printer (modified Model 33 Teletype).

The digital data were smoothed and converted to an ordinate linear in Raman shift rather than wavelength using the university's CDC-6500 computer and the Fortran program RAMAN¹² adapted from programs PC-180, PC-132, and PC-138 of R. N. Jones, *et al.*¹³

Frequency calibration was effected using mercury lines and the background plasma lines of the He-Ne and Ar⁺ lasers. The variation in response of the monochromator-detector system was examined using an NBS standard tungsten lamp reflected off of a MgO surface into the monochromator. Since the slit function and other parameters are not precisely known, the factor for normalization of intensities at appreciably different wavelengths will be less precise than the intensity values themselves.

Single-Crystal Spectra.—The optical setup used for the single-crystal measurements is illustrated in Figure 1. The 1270-mm lens was used to focus the beam to a diffraction limited point within the crystal. Since alignment of the optical components is critical in single-crystal spectroscopy, a large calcite crystal was used for checking the instrument's performance. Because of the rhombohedral structure of calcite, the spectra are simple, and excellent agreement between theory and experiment was observed with this compound by Porto, *et al.*¹⁴ From a sample of Iceland spar measuring $9 \times 10 \times 6$ cm purchased from Ward's Natural Science Establishment, Rochester, N. Y., a parallelepiped with dimensions $16 \times 21 \times 22$ mm was cut. With the aid of Laue back-reflection photographs, one face was ground perpendicular to the optic axis, another was perpendicular to one of the horizontal twofold axes, and a third was made perpendicular to these two faces. Final polishing was done using 1200- and 3200-grit abrasives. A smaller crystal measuring $3 \times 3 \times 6$ mm was cut similarly, polished, and mounted on a goniometer head. Alignment is believed to be better than $\pm 0.5^\circ$. As a test of optical alignment, the intensity of the forbidden I_{yz} component of the A_{1g} band (1085 cm^{-1}) in an $(yx)xy$ spectrum¹⁵ was

(7) C. W. Hobbs and R. S. Tobias, *Inorg. Chem.*, **9**, 1037 (1970).

(8) M. Goldstein and W. D. Unsworth, *J. Chem. Soc. A*, 2121 (1971).

(9) E. O. Schlemper and W. C. Hamilton, *Inorg. Chem.*, **5**, 995 (1966).

(10) H. M. Powell and D. Crowfoot, *Z. Kristallogr., Kristallgeometrie, Kristallphys., Kristallchem.*, **87**, 370 (1934).

(11) H. Gilman and R. G. Jones, *J. Amer. Chem. Soc.*, **68**, 517 (1946).

(12) We are indebted to Mr. J. W. Lundeen for writing this program.

(13) R. N. Jones, *NRC (Nat. Res. Council Can.) Bull.*, No. 11 (1968).

(14) S. P. S. Porto, J. A. Giordmaine, and T. C. Damen, *Phys. Rev.*, **147**, 608 (1966).

(15) The nomenclature of Damen, *et al.*, is used for the single-crystal experiments: T. C. Damen, S. P. S. Porto, and B. Tell, *ibid.*, **142**, 570 (1966).

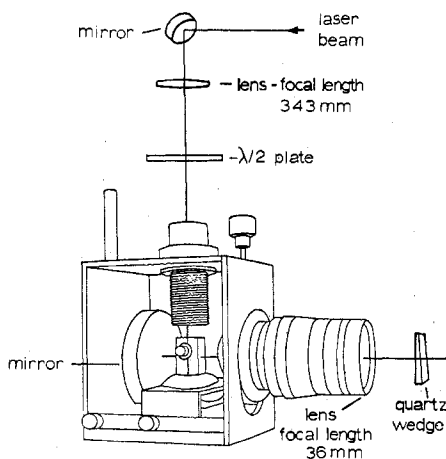


Figure 2.—Optical setup for measurements of depolarization ratios of solutions.

used. With the large crystal, He-Ne excitation, and a 3° collection angle, the forbidden intensity was reduced to the noise level; while with the small crystal, Ar^+ excitation focused with a 343-mm lens, and a somewhat larger collection angle, the forbidden band was comparable to the allowed bands in intensity. All of the single-crystal spectra were collected with He-Ne excitation. The equal intensities obtained for the 380-cm^{-1} band (E_g) from $x(yz)y$ and $x(zx)y$ spectra indicated that the quartz wedge effectively scrambled the polarization of the scattered light.

Before each set of measurements with a new crystal, the large calcite crystal was used to optimize the alignment and to test other spectrometer variables, e.g., polarization direction of the incident beam and the directions of the reference set of axes. With the small crystals, size limitations and optical inhomogeneities made it difficult to reproduce absolute intensities even when the same faces of a crystal were examined and all experimental conditions were unchanged. In view of these considerations, strict comparisons can be made only among relative intensities.

Intensities were measured as integrated areas. These were obtained by scanning slowly and recording pulse counts at 1-cm^{-1} intervals. The counts were summed over the band region, and the background was accounted for by subtracting the product of the number of data points and the average counts of ten points on either side of the band. Planimeter areas also were obtained from the analog displays.

Solution Spectra.—Solutions were contained in a ca. 0.9-ml double pass cell, and spectra were excited with the 5145 \AA line of an Ar^+ laser as illustrated in Figure 2. A 343-mm focal length lens was used to focus the laser beam to a diffraction limited point within the cell. The collection optics used a Kinotol F:1.5, 8-mm movie camera lens. No analyzer was used ($\rho = 0$; for depolarized lines). This is basically the scheme chosen by Claassen, *et al.*,¹⁶ as the best compromise among eight different setups for polarization measurements. Here it is improved by the use of the scrambler plate before the slit which removes the dependence of ρ on the monochromator characteristics. Intensities were measured as described above for the crystals. Scans were repeated a minimum of three times. The depolarization ratio of ν_1 of CCl_4 at 459 cm^{-1} was measured as a check on alignment of the apparatus. The observed value of ρ was 0.026; $\rho_{\text{theory}} = 0$ for an isolated, tetrahedral molecule. Very careful measurements of liquid CCl_4 gave $\rho = 0.0039$.¹⁷ Since an isotropic scatterer provides the most stringent test of the apparatus, the error due to instrumental effects should be within the range $0 \leq \delta\rho \leq 0.02$.

Results

Single-Crystal Spectra. Dimethyltin Difluoride.—

The space group is $I4/mmm$ (D_{4h}^{17}), and there are two formula units in the primitive cell.⁹ Neutron diffrac-

tion measurements indicated free rotation of the methyl groups at room temperature.¹⁸ For the discussion of the modes below 600 cm^{-1} , the methyl groups will be treated as single masses since normal-coordinate analyses on similar dimethyltin(IV) compounds have shown this to be a good approximation.⁷ Goldstein and Unsworth⁸ have given the representation for the crystal modes, and this information is summarized in Table I.

TABLE I
DERIVATION OF THE CRYSTAL FUNDAMENTALS OF $(\text{CH}_3)_2\text{SnF}_2$
BY THE CORRELATION METHOD

	Site symmetry species containing translation	$(\text{CH}_3)_2\text{SnF}_2$ D_{4h}^{17} factor group species
Tin atom	A_{2u}	A_{2u}
D_{4h} site group	E_u	E_u
2 carbon atoms	$2A_1$	A_{1g}
C_{4v} site group		A_{2u}
	$2E$	E_g
		E_u
2 fluorine atoms	$2B_{1u}$	A_{2u}
D_{2h} site group		B_{2u}
	$2B_{2u}$	$2E_u$
	$2B_{3u}$	

$$\Gamma_{\text{acoustic}} = A_{2u} + E_u$$

$$\Gamma_{\text{crystal}} = A_{1g} + E_g + 2A_{2u} + B_{2u} + 3E_u$$

$$\Gamma_{\text{internal skeletal}}((\text{CH}_3)_2\text{Sn}^{2+} (D_{3d} \text{ point group})) = A_{1g} + A_{2u} + E_u$$

It should be noted that the use of the D_{3d} point group for $(\text{CH}_3)_2\text{Sn}^{2+}$ is strictly correct only for the staggered conformer with a high rotational barrier. For the free ion with a negligible barrier to rotation of the methyl groups, a conventional point group cannot be employed to classify completely the rotorvibrational states.¹⁹ For structures of this type, the double group G_{36}^+ is required.²⁰ Recently Hall²¹ has discussed this for $(\text{CH}_3)_2\text{M}$ structures. Perhaps the most significant effect is that the treatment in the G_{36}^+ double group predicts Raman activity for the skeletal bending mode which is allowed for a rigid eclipsed structure but forbidden for the staggered conformer.

The single-crystal spectra below 1300 cm^{-1} are illustrated in Figures 3 and 4. All together, five bands⁷ at 144, 531, 1210, 2928, and 3021 cm^{-1} are observed of which the three higher frequencies correspond to internal vibrations of the methyl groups.

The Raman tensors for A_{1g} and E_g modes in factor group D_{4h}^{17} have the forms shown in (1) where $a =$

$$A_{1g} \begin{pmatrix} a & 0 & 0 \\ 0 & a & 0 \\ 0 & 0 & b \end{pmatrix}; \quad E_g \begin{pmatrix} 0 & 0 & e \\ 0 & 0 & 0 \\ e & 0 & 0 \end{pmatrix}, \begin{pmatrix} 0 & 0 & 0 \\ 0 & 0 & e \\ 0 & e & 0 \end{pmatrix} \quad (1)$$

$\alpha_{xx}' = \alpha_{yy}'$, $b = \alpha_{zz}'$, and $e = \alpha_{xz}' = \alpha_{zx}' = \alpha_{yz}' = \alpha_{zy}'$. The 531-cm^{-1} vibration clearly has A_{1g} symmetry, and the 144-cm^{-1} vibration has E_g symmetry as assigned by Goldstein and Unsworth⁸ from the powder spectra.⁷

For the 531-cm^{-1} band, large I_{zz} and weaker I_{xx} (or I_{yy}) were observed in $x(zz)y$ and $z(xx)y$ orientations.

(18) J. J. Rush and W. C. Hamilton, *Inorg. Chem.*, **5**, 2238 (1966).

(19) H. C. Longuet-Higgins, *Mol. Phys.*, **6**, 445 (1963).

(20) See the discussion and references in P. R. Bunker, *J. Chem. Phys.*, **47**, 718 (1967).

(21) J. R. Hall in "Essays in Structural Chemistry," A. J. Downs, D. A. Long, and L. A. K. Staveley, Ed., Plenum Press, New York, N. Y., 1971, Chapter 17.

(16) H. H. Claassen, H. Selig, and J. Shamir, *Appl. Spectrosc.*, **23**, 8 (1969).

(17) W. F. Murphy, M. V. Evans, and P. Bender, *J. Chem. Phys.*, **47**, 1838 (1967).

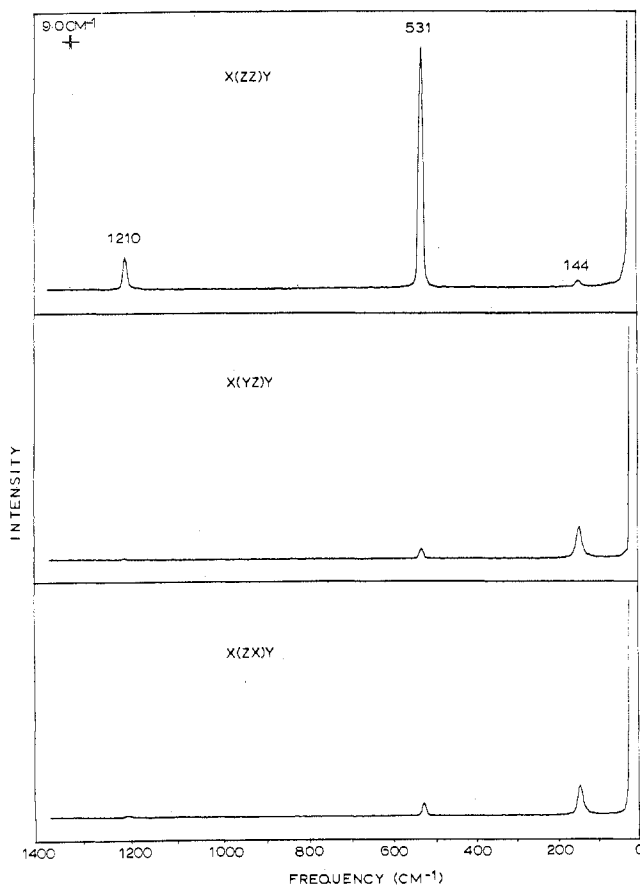


Figure 3.—Single-crystal Raman spectra of $(\text{CH}_3)_2\text{SnF}_2$ in $x()y$ geometry. Exciting line 6328 \AA , gain 2×10^3 cps, scan rate 9 \AA min^{-1} (ca. $22 \text{ cm}^{-1} \text{ min}^{-1}$), time constant 2 sec, slits $750 \times 900 \times 750 \mu$ (ca. 9 cm^{-1}).

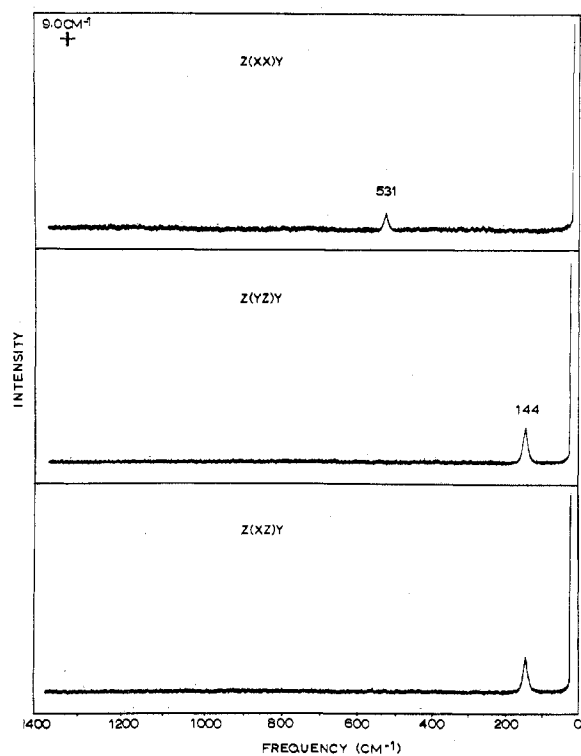


Figure 4.—Single-crystal Raman spectra of $(\text{CH}_3)_2\text{SnF}_2$ in $z()y$ geometry. Scan conditions are the same as in Figure 3, except for gain = 5×10^2 cps.

Low-intensity scattering was observed in the $x(yz)y$, $x(zx)y$, and $x(yx)y$ orientations, respectively; see Figure 3. The appearance of these forbidden intensities is not surprising; the observation of nonzero intensity I_{xy} for the symmetric vibration of calcite at 1085 cm^{-1} is analogous. This was appreciable with the $3 \times 3 \times 6$ mm calcite crystal, but it was imperceptible in the spectra of the $16 \times 21 \times 22$ mm crystal indicating the desirability of large single crystals. Because large single crystals of $(\text{CH}_3)_2\text{SnF}_2$ could not be grown, several small crystals were examined. The ratio of the intensity of the forbidden I_{xz} or I_{yz} component to I_{zz} was found to vary from one crystal to another, and the minimum values of I_{yz}/I_{zz} and I_{xz}/I_{zz} were 0.02 and 0.04, respectively.

Birefringence effects do not present any difficulty because of the very small differences between the ordinary and extraordinary indices of refraction. These were measured by the immersion method, and ω and ϵ were found to be 1.4940 and 1.5005 at the sodium D line. In the measurements where the laser beam was propagated along the crystal z axis, the scattered light was collected from one of the narrow faces of the crystal; and this is responsible for the low intensity of the spectrum.

The band at 144 cm^{-1} was observed to have the components I_{yz} and I_{xz} . The spectra in Figure 4 unequivocally define E_g symmetry. Weak scattering was measured in $x(yx)y$ and $x(zz)y$ orientations, and these are clearly forbidden intensities. The ratio of I_{zz} to I_{xz} or I_{yz} , see Figure 3, ranged from 0.09 to 0.35 and was observed to be lowest with the relatively thickest crystal.

Since the methyl groups are freely rotating at room temperature¹⁸ in a potential well with axial symmetry, the free ion internal methyl modes of A_{1g} and E_g symmetry should correlate with A_{1g} and E_g factor group modes. In the double group G_{36}^+ , these are of species A_{1g} and E_{2d} .²¹ Raman bands assignable to these methyl vibrations are observed at 3021 (antisymmetric stretching— E_g for free ion), 2921 (symmetric stretching— A_{1g} for free ion), and 1210 cm^{-1} (symmetric deformation— A_{1g} for free ion).

The observation for the 1210-cm^{-1} band of a measurable I_{zz} and zero I_{xz} , I_{yz} , and I_{yx} components is consistent with A_{1g} factor group symmetry. Scans with the $z(xx)y$ geometry did not show this band indicating that α_{xx} must be small compared to α_{zz} . Similarly, the band at 2928 cm^{-1} was observed to have finite intensity only in $x(zz)y$ geometry. The 3021-cm^{-1} band is quite low in intensity, and this coupled with the poor response of the photomultiplier at 7820 \AA made it impossible to record meaningful intensities for this asymmetric C-H stretching band with different crystal orientations.

The results of the intensity measurements on the 531- and 144-cm^{-1} bands are summarized in Tables II and III. The integrated areas in net photon pulse counts are believed to be more accurate than planimeter areas for measuring the intensities of weak bands, so only the former are reported. For stronger bands, the relative intensities obtained from either method were found to be in close agreement. In any one crystal orientation, e.g., $x()y$, I_{zz} of the 531-cm^{-1} band and I_{xz} and I_{yz} of the 144-cm^{-1} band were successively scanned; then this was repeated two to four times.

TABLE II
SINGLE-CRYSTAL RAMAN INTENSITY DATA FOR (CH₃)₂SnF₂: *x*()*y* GEOMETRY^a

Crystal	$\bar{\nu} = 531 \text{ cm}^{-1}$				$\bar{\nu} = 144 \text{ cm}^{-1}$			
	<i>x</i> (<i>zz</i>) <i>y</i>	<i>x</i> (<i>zx</i>) <i>y</i> ^b	<i>x</i> (<i>yz</i>) <i>y</i> ^b	<i>x</i> (<i>yx</i>) <i>y</i> ^b	<i>x</i> (<i>zz</i>) <i>y</i> ^b	<i>x</i> (<i>zx</i>) <i>y</i>	<i>x</i> (<i>yz</i>) <i>y</i>	<i>x</i> (<i>yx</i>) <i>y</i> ^b
No. 1 (3 × 3 × 1.5 mm) ^c	177 ± 2	16.7	7.2	2.2	7.4	29 ± 1	27.6 ± 0.6	4.1
No. 1	30.2	1.4	0.6	0	0.43	4.8	5.0	0.4
No. 1	284 ± 10	22.4	8.5	2.4	4.8	44.2 ± 0.6	41.1 ± 0.3	4.0
No. 2 (2 × 2 × 1 mm) ^c	273 ± 4	29.1	30.6	4.8	13.7	44.5 ± 0.5	44.4 ± 0.5	7.5
No. 3 (3 × 4 × 1.5 mm) ^c	276.9 ± 0.5	17.5	10.3	2.4	7.5	46.8 ± 0.2	49.3 ± 0.7	3.0

^a 6328-Å excitation. Net counts × 10⁻³. ^b Ideally should be zero. ^c Lengths along *x*, *y*, and *z* axes, respectively.

TABLE III
SINGLE-CRYSTAL RAMAN INTENSITY DATA FOR (CH₃)₂SnF₂: *z*()*y* GEOMETRY^a

Crystal	$\bar{\nu} = 531 \text{ cm}^{-1}$				$\bar{\nu} = 144 \text{ cm}^{-1}$			
	<i>z</i> (<i>xx</i>) <i>y</i>	<i>z</i> (<i>zx</i>) <i>y</i> ^b	<i>z</i> (<i>yz</i>) <i>y</i> ^b	<i>z</i> (<i>yx</i>) <i>y</i> ^b	<i>z</i> (<i>xx</i>) <i>y</i> ^b	<i>z</i> (<i>zx</i>) <i>y</i>	<i>z</i> (<i>yz</i>) <i>y</i>	<i>z</i> (<i>yx</i>) <i>y</i> ^b
No. 1 (3 × 3 × 1.5 mm) ^c	2.96 ± 0.10	1.33	1.21	0.80	0	10.8 ± 0.4	9.9 ± 0.1	0.80
No. 2 (2 × 2 × 1 mm) ^c	3.7 ± 0.2	2.4	2.2	0	0	12.1 ± 0.5	10.2 ± 0.05	1.3
No. 4 (3 × 3 × 0.5 mm) ^c	5.3 ± 0.3	1.0	1.4	0	0.5	16.9 ± 0.3	16.9 ± 0.2	1.3
No. 4	3.97 ± 0.09	0.76	0.53	0	0.27	14.1 ± 0.4	12.8 ± 0.7	0

^a 6328-Å excitation. Net counts × 10⁻³. ^b Ideally should be zero. ^c Lengths along *x*, *y*, *z* axes, respectively.

Using both the data from integration of the digital data and planimeter areas from earlier measurements, average values of $I_{zz,531}/I_{zz,yz,144} = 6.15 \pm 0.12$ and $I_{xx,531}/I_{xx,yz,144} = 0.31 \pm 0.01$ were obtained. From these data, the ratio $I_{zz}/I_{xx} = 19.8 \pm 0.6$. Since the Raman intensity is proportional to the square of the polarizability derivative, $|\alpha_{zz}'/\alpha_{xx}'| = 4.45 \pm 0.07$. If only the data considered to be most accurate, *i.e.*, those which have the lowest forbidden intensities, are used in the calculation, $I_{zz}/I_{xx} = 19.3 \pm 0.6$ and $|\alpha_{zz}'/\alpha_{xx}'| = 4.40 \pm 0.07$. This value is believed to be closer to the true value than that calculated from the averages. Since the derived polarizability tensor components are proportional to the square root of the intensity, only the absolute values are obtained. The tetragonal symmetry of the crystal requires that $\alpha_{zz}' = \alpha_{yy}'$, but these may be of the same or opposite sign from α_{zz}' . The derived polarizability tensor for the 531 cm⁻¹ A_{1g} vibration has the form shown in (2). The

$$\begin{pmatrix} \pm 1.00 & 0 & 0 \\ 0 & \pm 1.00 & 0 \\ 0 & 0 & \pm 4.40 \pm 0.07 \end{pmatrix} \quad (2)$$

form of the Raman tensors for the 144 cm⁻¹ E_g mode relative to the A_{1g} tensor can be calculated in the same way. Taking α_{zz}' , A_{1g} = 4.40 ± 0.07 the values of α_{zz}' and α_{yz}' , E_g, were found to be 1.77 ± 0.01. An approximate correction for the variation in spectrophotometer sensitivity with frequency, $\sigma_{531}/\sigma_{144} = 1.14$ can be applied to put the E_g tensor components on the same basis as those for the A_{1g} tensor. The corrected E_g components are $\alpha_{zz}' = \alpha_{xx}' = \alpha_{yy}' = \alpha_{yz}' = 1.55$. As noted in the Experimental Section, the correction factor is less accurate than the intensity measurements.

Dimethylthallium Bromide.—This compound crystallizes in space group *I4/mmm* (*D*_{4h}¹⁷), *Z* = 2.¹⁰ The primitive cell contains one formula unit. The representation for the optical modes is summarized in Table IV.

As was the case for (CH₃)₂SnF₂, (CH₃)₂TlBr should exhibit only two Raman bands below 600 cm⁻¹. The

TABLE IV
DERIVATION OF THE CRYSTAL FUNDAMENTALS OF (CH₃)₂TlBr BY THE CORRELATION METHOD

Site symmetry species containing translation	(CH ₃) ₂ TlBr <i>D</i> _{4h} ¹⁷ factor group species
Thallium atom	A _{2u} ————— A _{2u}
<i>D</i> _{4h} site group	E _u ————— E _u
2 carbon atoms	2A ₁ ————— A _{1g}
<i>C</i> _{4v} site group	————— A _{2u}
	2E ————— E _g
	————— E _u
Bromine atom	A _{2u} ————— A _{2u}
<i>D</i> _{4h} site group	E _u ————— E _u

$\Gamma_{\text{acoustic}} = A_{2u} + E_u$

$\Gamma_{\text{crystal}} = A_{1g} + E_g + 2A_{2u} + 2E_u$

$\Gamma_{\text{internal skeletal}}((\text{CH}_3)_2\text{Tl}^+ (D_{3d} \text{ point group})) = A_{1g} + A_{2u} + E_u$

spectra are illustrated in Figure 5. Single-crystal spectra could be obtained with only one crystal orientation, *i.e.*, with the laser beam propagating along the *z* axis. The (010) and (100) faces were too narrow to permit accurate intensity measurements with other orientations. The band at 96 cm⁻¹ in the *z*(*zx*)*y* orientation does not appear in the *z*(*xx*)*y* orientation, and it is unambiguously the E_g mode. The Tl-C stretching vibration at 488 cm⁻¹ has large *I*_{xx} and weak *I*_{zz} components; the latter is forbidden and arises from α_{zz}' . The intensity of this band was high in the *x*(*zz*)*y* orientation, but the intensities of *x*(*zx*)*y* and *x*(*yz*)*y* also were appreciable because of the thinness of the crystals. Nevertheless, this mode clearly has A_{1g} symmetry.

Raman Spectra of Aqueous Solutions of (CH₃)₂Sn(ClO₄)₂ and (CH₃)₂TlClO₄.—The solutions contain aquated (CH₃)₂Sn²⁺ or (CH₃)₂Tl⁺ and perchlorate ions, and their spectra have been recorded previously with mercury arc excitation. This precluded accurate measurements of the depolarization ratios, and McGrady and Tobias²² gave $\rho_{\text{unior}} = 0.444$ for the 529-cm⁻¹ A_{1g} Sn-C stretching mode of (CH₃)₂Sn²⁺. Goggin

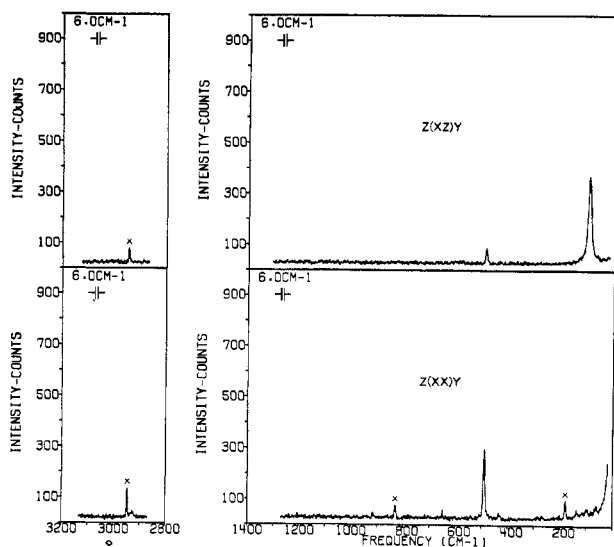


Figure 5.—Digitally collected single-crystal Raman spectra of $(\text{CH}_3)_2\text{TiBr}$ in $z(x)y$ geometry. Exciting line 6328 \AA , scan rate 9 \AA min^{-1} (ca. $22 \text{ cm}^{-1} \text{ min}^{-1}$), data collected at 0.5 \AA —approximately 1.2 cm^{-1} intervals, slits $750 \times 900 \times 750 \mu$ (ca. 9 cm^{-1}). The bands marked with x are background plasma lines of the He-Ne laser.

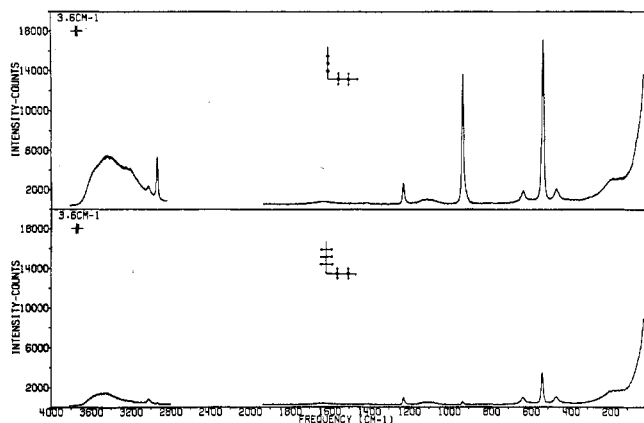


Figure 6.—Digitally collected Raman spectra of aqueous $1 M (\text{CH}_3)_2\text{Sn}(\text{ClO}_4)_2$. Exciting line 5145 \AA , scan rate 9 \AA min^{-1} (ca. $34 \text{ cm}^{-1} \text{ min}^{-1}$), data collected at 0.5 \AA —approximately 1.8 cm^{-1} intervals, slits $200 \times 400 \times 200 \mu$ (ca. 3.6 cm^{-1}).

and Woodward²³ only reported the $496\text{-cm}^{-1} A_{1g}$ Ti-C stretching mode of $(\text{CH}_3)_2\text{Ti}^+$ as polarized. Figure 6 shows digital, computer plotted spectra of $1 M$ aqueous $(\text{CH}_3)_2\text{Sn}(\text{ClO}_4)_2$. The computed depolarization ratio, ρ , was 0.22 ± 0.02 .

In addition to permitting the accurate measurement of depolarization ratios, the laser Raman spectrophotometer also makes it possible to obtain spectra closer to the exciting line. The low-frequency depolarized band at 176 cm^{-1} is clearly visible in the spectra.

Raman spectra of $0.3 M (\text{CH}_3)_2\text{TiClO}_4$ also were obtained, and the depolarization ratio for the $496 \text{ cm}^{-1} A_{1g}$ Ti-C stretching mode was found to be 0.22 ± 0.02 . This Ti-C stretching band was completely resolved from ν_4 of ClO_4^- at 461 cm^{-1} by using 1.1-cm^{-1} slits. The low-frequency depolarized band of the $(\text{CH}_3)_2\text{Ti}^+$ ion was observed at 96 cm^{-1} .

(23) P. L. Goggin and L. A. Woodward, *Trans. Faraday Soc.*, **56**, 1591 (1960).

Discussion

The derived polarizability tensor for the 531-cm^{-1} vibration of $(\text{CH}_3)_2\text{SnF}_2$ was given by (2). In the Wolkstein model²⁴ in which it is assumed that bond stretchings involve changes in polarizabilities which are localized in the bonds being stretched, α_{531} is just the tensor sum of the two derived Sn-C bond polarizability tensors. Consequently, the relative values of the components of $\alpha_{\text{Sn-C}}$ are given by α_{531} .

The locus of points formed by plotting, from a common origin, the end points of vectors representing the dipole moments induced by a unit electrical field defines the polarizability ellipsoid with axes denoted by x , y , and z .²⁵ This quantity is unknown for the $(\text{CH}_3)_2\text{SnF}_2$ crystal. Raman intensities are determined by $(\partial\alpha/\partial Q_j) = \alpha_j'$. In the case of the hydrogen molecule, the sign of α' was established as positive.²⁶ Consequently, the size of the polarizability ellipsoid should increase with bond elongation and decrease with bond shortening, *i.e.*, the ellipsoid breathes during a symmetric stretching vibration. Since a tensor component is obtained from the square root of an intensity, there is a sign ambiguity. The case with $\alpha_{xx}' = \alpha_{yy}'$ and α_{zz}' all of the same sign is believed to be the more likely, since in the case where the signs differ, the intensity of the symmetric stretching mode would approach zero in measurements with unoriented samples as α_{xx}' approached $\alpha_{zz}'/2$. With all diagonal elements of the same sign, the intensity for symmetric Sn-C stretching would be 7.08 times as large as when α_{xx}' and α_{yy}' differ from α_{zz}' in sign. Such metal-carbon stretching vibrations all have been observed to have very high Raman intensities. Secondly, in the calculation of α_{xx}' , α_{yy}' , and α_{zz}' for the corresponding vibration of $(\text{CH}_3)_2\text{Sn}(\text{acac})_2$,²⁷ the unique solution was found to give the same sign for the diagonal elements of α' .

When the individual components of the derived polarizability tensor are known, the tensor invariants $\bar{\alpha}' = 1/3(\alpha_{xx}' + \alpha_{yy}' + \alpha_{zz}')$ and $\gamma'^2 = 1/2[(\alpha_{xx}' - \alpha_{yy}')^2 + (\alpha_{yy}' - \alpha_{zz}')^2 + (\alpha_{zz}' - \alpha_{xx}')^2 + 6(\alpha_{xy}'^2 + \alpha_{xz}'^2 + \alpha_{yz}'^2)]$ can be computed. For an unoriented sample and the optical set up used in our experiments—polarized incident beam, 90° collection, and no analyzer—the depolarization ratio ρ is given by $6\gamma'^2/(45\alpha'^2 + 7\gamma'^2)$. Consequently, the depolarization ratio can be computed. For $(\text{CH}_3)_2\text{SnF}_2$, assuming α_{xx}' , α_{yy}' , and α_{zz}' all have the same sign, the appropriate values are $\bar{\alpha}' = 2.13 \pm 0.02$, $\gamma'^2 = 11.6 \pm 0.1$, and $\rho = 0.24 \pm 0.01$.

Since the two indices of refraction of $(\text{CH}_3)_2\text{SnF}_2$ were similar, 1.4940 and 1.5005, an attempt was made to measure depolarization ratios for the crystal using a powder sample mulled with a liquid of refractive index intermediate between the two crystal values. The compound proved to be too birefringent, however, and the light was effectively depolarized. A similar observation was reported by Johnson and Sutton²⁸ who obtained good ρ values with powders of isotropic but not of birefringent compounds.

(24) See the discussion by L. A. Woodward in "Raman Spectroscopy," H. A. Szymanski, Ed., Plenum Press, New York, N. Y., 1967, p 37.

(25) See, *e.g.*, H. A. Stuart, "Molekülstruktur," 3rd ed, Springer, Berlin, Heidelberg, New York, 1967, p 414.

(26) R. P. Bell, *Trans. Faraday Soc.*, **38**, 422 (1942).

(27) V. B. Ramos and R. S. Tobias, unpublished research.

(28) D. W. Johnson and D. Sutton, *Can. J. Chem.*, **49**, 671 (1971).

If the electron distribution in the $(\text{CH}_3)_2\text{Sn}^{\text{IV}}$ moiety is the same in different compounds and the vibrational modes examined involve only the Sn-C coordinates, then the derived polarizability tensors should be the same. This is, in fact, the basis for the assumption that α' values can be described in terms of meaningful derived bond polarizability tensors, *i.e.*, the Wolkenstein polarizability theory.²⁴ If the electron distribution in the bond changes from one molecule to another, if there are effects from lone pair electrons, or if there are significant nonbonded interactions, it should not be expected that α and α' can be obtained simply by summing over the bonds in the scatterer.

Previously, we have suggested⁷ that the interactions of the $(\text{CH}_3)_2\text{Sn}^{2+}$ moiety with fluoride ions in $(\text{CH}_3)_2\text{SnF}_2$ and with water in the case of $(\text{CH}_3)_2\text{Sn}^{2+}(\text{aq})$ were almost purely electrostatic. The Sn-C symmetric stretching vibration of the aqueous solution of $(\text{CH}_3)_2\text{Sn}(\text{ClO}_4)_2$ was found to have $\rho = 0.22 \pm 0.02$. Within the experimental error this is the same as the value computed for crystalline $(\text{CH}_3)_2\text{SnF}_2$, $\rho = 0.24 \pm 0.01$.

The value obtained for ρ with the aqueous solution of $(\text{CH}_3)_2\text{TlClO}_4$ was 0.22 ± 0.02 , the same as that obtained with the solution of $(\text{CH}_3)_2\text{Sn}(\text{ClO}_4)_2$. Since both of these ions should have axial symmetry in solution, the ratios $\alpha_{zz}'/\alpha_{xx}'$ must be very similar for both.

It should be noted that because of the general inverse relationship between the atomic polarizability and reciprocal of the ionization potential,²⁹ the atomic polarizability of thallium is predicted to be higher than that of tin. The Tl-C bond polarizability ellipsoid may be larger than that of the Sn-C bond, and the actual values of the α' components need not be similar.

In Table V, values are given for the ratios of the per-

TABLE V

RATIOS OF PERPENDICULAR AND LONGITUDINAL COMPONENTS OF BOND POLARIZABILITIES

Compd	α'_p/α'_l	Ref	Compd	α'_p/α'_l
CN ⁻	0.46	31	$(\text{CH}_3)_2\text{SnF}_2$	0.227 (Sn-C)
CH ₄	0.139	30	$(\text{CH}_3)_2\text{Sn}^{2+}(\text{aq})$	0.25 (Sn-C)
CCl ₄	0.46	31	$(\text{CH}_3)_2\text{Tl}^{2+}(\text{aq})$	0.25 (Tl-C)
PtF ₆ ²⁻	0.39	32		
SnCl ₆ ²⁻	0.55	33		
PtCl ₆ ²⁻	0.12	33		

pendicular, α'_p , and longitudinal components, α'_l , of several derived bond polarizabilities. The data for polyatomic scatterers, which all were determined

(29) T. Yoshino and H. J. Bernstein, *J. Mol. Spectrosc.*, **2**, 213 (1958).

with unoriented samples, have been obtained in several ways including measurement of Raman relative to Rayleigh intensity (CH_4),³⁰ the measurement of the intensities of $\nu_1(\text{A}_1)$ and ν_3 or $\nu_4(\text{F}_2)$ for CCl_4 ,³¹ and the determination of the relative intensities of $\nu_1(\text{A}_{1g})$ and $\nu_2(\text{E}_g)$ of the hexahalogenometalates.^{32,33} In the case of the colored PtF_6^{2-} and PtCl_6^{2-} , it has been suggested that a resonance effect led to an enhancement of the intensity of ν_2 relative to ν_1 .³⁴

Chantry and Plane³¹ concluded that α'_p/α'_l should be larger for multiple bonds, *e.g.*, in CN^- , than for single bonds. On the other hand, Woodward and Ware³² concluded that there was an inverse relationship between α'_p/α'_l and bond order for the hexahalides of tin(IV) and platinum(IV), although as noted above these values may be influenced by the resonance effect. Jones³⁵ suggested that increasing back bonding using metal d orbitals in linear dicyano complexes should decrease the ratio α'_p/α'_l . No consistent pattern emerges from the few data available. The ratio α'_p/α'_l is remarkably consistent for the two heavy metal-carbon bonds examined in this work which are examples of single σ bonds.

One interesting feature comes to light when solution and crystal spectra are compared. The Raman spectra of crystalline $(\text{CH}_3)_2\text{SnF}_2$ and aqueous $(\text{CH}_3)_2\text{Sn}^{2+}$ both show two bands at 531, 144 cm^{-1} and 529, 176 cm^{-1} , respectively. Similarly, crystalline $(\text{CH}_3)_2\text{TlBr}$ and aqueous $(\text{CH}_3)_2\text{Tl}^+$ both have two bands at 488, 96 cm^{-1} and 496, 96 cm^{-1} . In the crystals, the lower frequency mode is a rotatory lattice vibration. With these aquo ions, the low-frequency bands usually have been assigned to the infrared allowed C-Sn-C bending mode which was assumed to become Raman active by a breakdown of the free ion selection rules. As noted above, when free internal rotation is considered, the bending vibration is not Raman forbidden. Assignments to the bending vibration have been made for $(\text{CH}_3)_2\text{Sn}^{2+}$,²² $(\text{CH}_3)_2\text{Tl}^+$,²³ and $(\text{CH}_3)_2\text{Pb}^{2+}$.³⁶ These bands generally have quite appreciable intensity. Considering that the crystal modes are rotatory lattice vibrations, it seems quite likely that the modes observed with the aqueous solutions are librations, *i.e.*, rotations restricted by the solvation water which in turn is hydrogen bonded to the bulk solvent.

(30) Y. Yoshino and H. J. Bernstein, *J. Mol. Spectrosc.*, **2**, 241 (1958).(31) G. W. Chantry and R. A. Plane, *J. Chem. Phys.*, **33**, 634 (1960).(32) L. A. Woodward and M. J. Ware, *Spectrochim. Acta*, **19**, 775 (1963).(33) L. A. Woodward and J. A. Creighton, *ibid.*, **17**, 594 (1961).

(34) See the discussion in ref 10, p 151.

(35) L. H. Jones, *Spectrochim. Acta*, **19**, 1675 (1963).(36) C. E. Freidline and R. S. Tobias, *Inorg. Chem.*, **5**, 354 (1966).